Atmospheric Environment 45 (2011) 5612–5620

Contents lists available at ScienceDirect

Atmospheric Environment

journal homepage: www.elsevier.com/locate/atmosenv

Characterization of macromolecular organic matter in atmospheric dust from Guangzhou, China

Jinping Zhao [a,b], Ping'an Peng [a,*], Jianzhong Song [a], Shexia Ma [a], Guoying Sheng [a], Jiamo Fu [a]

[a] State Key Laboratory of Organic Geochemistry, Guangzhou Institute of Geochemistry, Chinese Academy of Sciences, Guangzhou 510640, PR China
[b] Institute of Urban Environment, Chinese Academy of Sciences, Xiamen 361021, PR China

ARTICLE INFO

Article history:
Received 13 November 2010
Received in revised form
9 April 2011
Accepted 15 April 2011

Keywords:
Falling dust
Chemical compositions
Organic macromolecules
Elemental analysis
^{13}C-CP/MAS NMR

ABSTRACT

The chemical compositions of organic macromolecules in dust are very complex and have not yet been investigated in detail. In this paper, we study the organic macromolecules in 12 dust samples collected from an urban and suburban area of Guangzhou, China. Organic macromolecules in the dust were firstly separated into humic acids (HA), kerogen and black carbon (KB) and black carbon (BC) fractions by chemical treatment with NaOH, HCl/HF and $K_2Cr_2O_7/H_2SO_4$, respectively. The isolated fractions were subsequently characterized using elementary analysis (EA), organic petrographic examination (OPE), scanning electron microscopy (SEM), and solid state ^{13}C cross-polarization and magic angle spinning nuclear magnetic resonance spectroscopy (^{13}C-CP/MAS NMR) etc. The results showed that the major organic macromolecules were KB, which accounted for 64.8%–95.8% of total organic carbon (TOC) in the dusts. Isolated HAs were characterized by high H/C, N/C and O/C atomic ratios, and high carboxyl, methoxyl and aliphatic carbon contents in the overall carbon structure; meanwhile, kerogens (K) showed lower H/C, N/C and O/C atomic ratios than those of HAs and had chemical compositions enriched in hydroxyl carbon; further, the optical features of K were similar to those of "vitrinite". BC is formed from the combustion of biomass and fossil fuels, so that aromatic and aliphatic carbons are the most important components in its carbon skeleton. Under the microscope, BC appeared to belong to the petrographic groups, such as "semifusinte" and "fusinite", and showed a distinct texture when observed by SEM. Compared with the HAs and K isolated from soils and sediments, HAs in dust were relatively lower in aromatic carbon and K in dust was always "type III". These results are strongly consistent with the dust samples originating from the photochemical degradation of volatile organic compounds, in contrast to the geological HAs and K which are sourced from the biodegradation of lignin and algae or from bacterial activities in water and sediment.

1. Introduction

Atmospheric falling dust comprises particles which fall to the ground under the effect of gravitation. Generally, these particles have diameters between 10 μm and 100 μm. Although dust particles are larger than aerosols, they still act as important pollutants, carrying nutrients and toxic matter that can strongly influence biogeochemical cycles in the Earth surface system and that can harm vegetation and humans (Smith et al., 1996; Griffin et al., 2003; Prospero and Lamb, 2003; Kellogg et al., 2004; Weir-Brush et al., 2004; Griffin, 2005). The dust settling process, known as dry precipitation, removes materials such as organics, nitrates, sulfates and chlorinates from the atmosphere (Falkovich et al., 2004; Sullivan et al., 2007) and is one of the most important natural attenuation mechanisms that maintains the quality of the Earth's atmosphere.

Dust comprises very complex chemical constituents. The characterization of the composition of dust will help us to better understand its geochemical behavior in the atmosphere. Moreover, chemical characterization of dust will increase our knowledge of aerosol, as dust is the end member of the range of particles classified as aerosol. Generally, the analysis of aerosol composition is difficult because the amount of aerosol that can be collected is always insufficient for such study. In the past, inorganic matter and low molecular weight organic matter in the dust have been studied in detail (Lee et al., 2007; Abed et al., 2009; Shen et al., 2009). However, studies of the macromolecular organic matter are limited, due to the lack of appropriate methodologies for fractionation and characterization.

The organic matter in atmospheric falling dust includes two classes of compounds: low molecular weight organic matter such

* Corresponding author.
E-mail address: pinganp@gig.ac.cn (Ping'an Peng).

1352-2310/$ – see front matter © 2011 Elsevier Ltd. All rights reserved.
doi:10.1016/j.atmosenv.2011.04.039

as organic acids, amino acids and polysaccharides, and macromolecules such as humic-like substances (hulis), humic acids (HA), kerogen (K) and black carbon (BC). The macromolecules generally account for more than 90% of organic matter in the dust (Mukai and Ambe, 1986; Zappoli et al., 1999) and are formed directly by particle emission or indirectly by photochemical oxidation, deoxidization and polymerization of volatile organic compounds (VOCs) in the atmosphere. Therefore, organic macromolecules in dust may contain very important signals related to their source and transformation processes. The detailed composition study is certainly of scientific importance.

Isolation and characterization of HA, K and BC in soils and sediments have been widely performed (Garcette-Lepecq et al., 2000; Simpson and Hatcher, 2004; Li et al., 2006). For example, Song et al. (2005) isolated HAs, K and BC from the soils and sediments in the Pearl River Delta area. HAs are mainly composed of aromatic cores bridged by aliphatic and functional groups (Li et al., 2004; Song et al., 2005) while K contains aliphatic and aromatic entities. BC consists mainly of aromatic carbon with a rigid structure. Oxygen functional groups are present on the surface of BC particles. The characterization of macromolecules yields a general picture of the chemical structure of organic matter in soils and sediments.

As yet, these isolation and characterization approaches have not been applied to dust, although hulis and BC in aerosol have been widely studied in the past (Havers et al., 1998; Krivácsy et al., 2000; Dinar et al., 2006; Taraniuk et al., 2007; Kirchstetter et al., 2008; Dutkiewicz et al., 2009; Sýkorová et al., 2009). In the present study, we isolated HAs, kerogen and black carbon (KB) and BC from dust collected in Guangzhou, China, and then characterized the chemical composition of the fractionated macromolecule organic matter using elementary analysis (EA), X-ray diffraction (XRD), organic petrographic examination (OPE), scanning electron microscopy (SEM), solid state ^{13}C cross-polarization and magic angle spinning nuclear magnetic resonance spectroscopy (^{13}C-CP/MAS NMR) and Fourier transformed infrared spectroscopy (FTIR). The aim of this study is to provide new chemical information about organic macromolecules in dust.

2. Materials and methods

2.1. Sampling

Dust samples were collected from two sites in Guangzhou city: Wushan in Tianhe district and the university town in Panyu district.

Wushan (WS) represents an urban area and is surrounded by highways, schools, residential and office buildings, and industrial factories. The main sources of air pollution at this site are thought to be anthropogenic. Samples were collected on the roof of a library building that is 18 m above the ground.

The university town (UT) represents a suburban area located at the boundary between urban and rural areas and is surrounded by several universities. The main sources of air pollution at this site are a mixture of anthropogenic and biological. Samples were collected on the roof of a five-story building in South China Normal University at 23 m above the ground.

Roofs selected for sampling sites were cleaned before sampling. Neither site received any rain, but allowed atmospheric dust to fall to the ground under its own gravitation. The sampling sites were high enough to avoid contamination by secondary dust raised from the ground. The sampling sites were cleaned after individual sampling periods, prior to collection of the next sample. Sampled dust was pre-cleaned by 0.28 mm sieve and then stored in a brown bottle within desiccators before use. Falling dust was collected at intervals of 2 months at WS and the UT between April 2006 and May 2007. Sampling lasted one year and in total 12 samples were collected.

2.2. Fractionation of macromolecular organic matter

The isolation protocol of macromolecular organic matter including HA, KB and BC was based on that of Song et al. (2002). Briefly, HA, KB and BC were separated from the dust by treatment with NaOH, HCl/HF and $K_2Cr_2O_7/H_2SO_4$. The detail procedures please see the Supplementary Materials.

2.3. EA

C, H, O and N contents of the HA, KB and BC fractions were measured using an Elementar Vario EL III elemental analyzer (Hanau, Germany). Before analysis, the samples were decarbonated using 0.5 M HCl. The TOC values listed in Table S1 (See Supplementary Materials) are the averages of three sample measurements.

2.4. XRD

A standard powder X-ray diffraction method was used to determine the mineral species that had not been removed during the demineralization process and to estimate the interplanar spacing of aromatic sheets of organic matrices. XRD tests were conducted on a Japan D/MAX-IIIA powder diffractometer with a Bragg-Bentano θ:2θ configuration, using a Cu target tube and a graphite monochromator. Samples were analyzed within the range 10–70°, tube voltage 10 kV, tube flow 30 mA, scan rate 10° min^{-1}, and wide sampling step 0.02°.

2.5. OPE

The organic facies, and the shapes, sizes and colors of the fractionated macromolecules were examined under optical microscopy (Leitz MPV-3) in three different light modes: transmitted, reflected and fluorescent; the last was induced by blue excitation (546 nm). The thin sections used for examinations in transmitted modes were prepared by evenly spreading sample powders on glass slides, which were then cemented with glycerol and covered with a cover glass. The polished sections used for reflected and fluorescent modes were prepared by spreading sample powers on porcelain slides and cementing the powders with low-fluorescence 502 mucilage glue. The slides were then thin-sectioned and polished.

2.6. SEM

The shapes, sizes and morphologies of HAs, KBs and BCs were examined using a Japan S-3700N scanning electron microscope with Oxford Link INCA 300 energy-dispersive X-ray spectrometer.

2.7. Solid state CP/MAS ^{13}C NMR spectroscopy

The functionalities of the isolated fractions were determined by solid-state ^{13}C NMR spectroscopy using a Bruker DRX-400 (Switzerland) on a 4 mm probe at 100.63 MHz carbon frequency with cross-polarization/magic angle spinning (CP/MAS). The rotor was made of zirconia with a Kel-F cap. The signals were recorded at 1 ms cross-polarization contact time and approximately 1000 data points were obtained for each sample. The time periods for signal acquisition for a given sample varied from 1 to 10 h.

2.8. FTIR spectroscopy

The isolated fractions were mixed with potassium bromide at a sample to potassium bromide ratio of 1:10, ground, and pressed into a thin slice. Finally, the prepared sample slice was fitted in the

sample chamber and analyzed by FTIR spectroscopy (Bruker-Vector 33, Germany).

3. Results and discussion

3.1. Contents and elemental compositions of HA, KB and BC

The relative contents of HA, KB and BC were calculated as an organic carbon content based on the following measures: (1) weight of a given isolated fraction (W_{f_i}); (2) TOC content of the fraction (TOC_{f_i}); (3) weight of the original sample from which the given fraction was isolated (W_{f_o}); and (4) TOC content of the original sample (TOC_{f_o}). These values were substituted into the following equation:

$$F_i = \frac{TOC_{f_i} \times W_{f_i}}{TOC_{f_o} \times W_{f_o}} \times 100$$

The average value of F_i% was calculated from the determinations of three triplicate samples, and the relative standard deviations were less than 5%. The final results of the relative contents of different fractions are summarized in Table S1.

The data listed in Table S1 indicate that: (1) HA and KB contain 84.60–102.60% of the TOC, while lost carbon, equivalent to 5.28–28.18% of TOC, may comprise the fulvic acids that are soluble in water; (2) particulate KB constitutes 64.08–89.72% of the TOC, of which K and BC comprise 41.51–60.76% and 25.22–33.32% of the TOC, respectively; and (3) the elemental compositions of HA, KB and BC differ drastically. These results tell us that the most important constituent of macromolecules is KB. K appears to be more important than hulis in the dust.

The BC contents presented in Table S1 are comparable to those reported in the literature. For instance, BC was reported to account for 10.1–41.3% of TOC for total suspended particle (TSP) (Salama et al., 2003), 5–39% of TOC in lake sediments from France (Lim and Cachier, 1996), and 4.14–17.30% of TOC in Pearl River Delta sediments and soil in China (Ran et al., 2007). The high BC in the samples indicated that anthropogenic input can be an important source of organic matter in dust from industrialized regions.

The major errors in relative contents HA, K and BC in Table S1 may be attributed to the loss of fine particles during decantation of supernatant after base extraction, oxidation of BC particles, and incomplete digestion of K by dichromate. During the base extraction, dispersed dark-colored fine particles that are presumably BC or K materials were sometimes observed on the surface of the solution after centrifugation for several hours, likely due to their surface hydrophobicity and low bulk density. Elemental analyses of kerogen and BC standards after NaOH treatment show that such particles contribute <4% of KB in the TOC. The loss of fine particles during base extraction may therefore be neglected. To assess the completion of kerogen oxidation, three isolated BC samples were re-treated with dichromate/sulfuric acid solution. Less than 6% of the TOC reduction of all isolated BC samples was observed in these repeats, suggesting that K was completely digested and that the oxidation of fine BC particles may be limited during the last step of the procedure. Thus, all data shown in Table S1 are found to be robust and may be used to interpret the composition of organic macromolecules in the dust.

Fig. 1 clearly shows that the O/C and H/C atomic ratios decrease in the order HA > K > BC. These ratios, when plotted on the van Krevelen diagram, indicate that all fractions lie approximately on the line of an atomic H/O ratio of 5:1. HAs isolated from WS dust have O/C and H/C atomic ratios of 0.32–0.36 and 1.40–1.61, while HAs from the UT dust show slightly higher O/C and H/C atomic ratios, i.e., 0.32–0.39 and 1.52–2.06, respectively. Even though only a few sample were analyzed, HAs from winter samples collected in WS show slightly higher H/C atomic ratios than those from summer. Compared with H/C and O/C atomic ratios of HAs from soils, HAs from dust are relative high in H/C and low in O/C (Mafra et al., 2007). However, the K isolated from the dust has much lower H/C and O/C ratios and is typical type III K, in contrast to geological K. Similarly to the HA fraction, K from the UT shows relatively high H/C. The BC fractions isolated from WS and the UT are similar in terms of atomic O/C and H/C ratios, which are 0.08–0.11 and 0.45–0.60, respectively. These ratios were slightly lower than the H/C and O/C atomic ratios of BC in soil and sediment, similar to the H/C and O/C atomic ratios in modern BC and standard reference BC (Song et al., 2002; Hammes et al., 2008), and consistent with the H/C and O/C atomic ratio in charcoal plant debris (Goldberg, 1985).

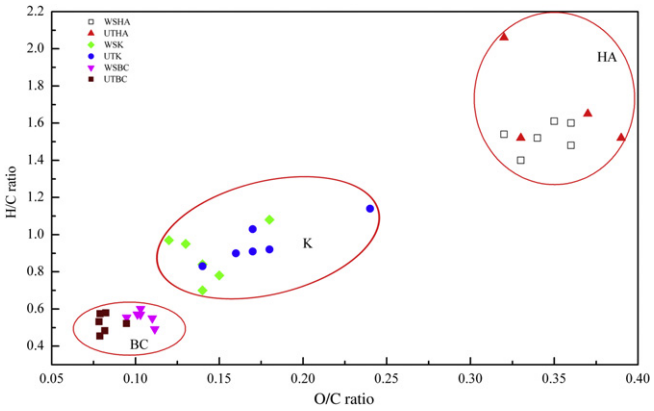

Fig. 1. A van Krevelen plot of HAs, K and BC isolated from 12 dust samples. Atomic ratios of Ks were calculated based on data for KB and BC in Table S1. Note: samples were named according to site and fractions as given in Table S1. For example, WSHA includes 6 HA fractions that were isolated from 6 corresponding dust samples in WS between 2006 and 2007.

The N/C ratios listed in Table S1 indicate that most nitrogen was combined into the HA fractions, with very little nitrogen present in the KB fraction.

The variations of elemental C, H, N and O in macromolecular fractions in dust can be explained by the source and transformation process of organic matter. HA and K fractions in dust were derived from photochemical oxidation of VOCs, which can be either anthropogenic or biogenetic. However, BC is mainly emitted from fossil fuels and biomass combustion. Moreover, K in the dust can be recognized as the product of further oxidation of HA or the inter-molecular combination of HA. This hypothesis provides a good explanation for the order of H/C, N/C and O/C ratios in HA, K and BC (Fig. 1). VOCs first form HA by oxidation in the air; here the H/C, O/C and N/C ratios are highest. BC originates from combustion, where most O, N and H are lost, therefore those ratios are lowest. Further oxidation of HA or inter-molecular combination will lose CO_2, H_2O and NO_x, so that the ratios are intermediate. This hypothesis also can explain the H/C and O/C ratios in WS and UT. UT is located in a suburban environment, where there is more HA and K derived from biogenetic VOCs. Hence, those ratios are relatively higher.

In comparison with geological HA, we find that HA contents in dust have higher N/C and H/C ratios. This could be attributed to the different sources of the two HAs. HAs in soils were derived from humification of lignin material, and have low H/C ratios. In the humification process, most nitrogen compounds (such as proteins) are degraded by micro-organisms. Therefore, they show low H/C and N/C ratios. Meanwhile, HAs from dust originated from oxidation reactions between NOx and VOCs. Some VOCs are from isoprenoids and terpenoids, which have high H/C ratios. In this process, many nitrogen compounds can be formed. Therefore, higher H/C and N/C ratios can be expected in HAs extracted from the dust.

The discrepancy regarding K sources can also explain the differences between kerogen contents in dust and sediments. The former is formed by oxidation, during which most H is lost. Therefore, K is always present as type III. However, the sources of geological K are diverse, and can originate not only from biodegradation products of algae, bacteria and plants but also from reworked organic matter such as in the weathering products of organic matter and biomass burning-related BC. Hence, sedimentary K may be types I, II or III depending on the geological environment in which the K was deposited.

3.2. XRD

Fig. 2 shows the XRD spectra of KB and BC isolated from dust in WS and UT. The inorganic minerals which have been detected previously in falling dust (see Zhao et al., 2010) were not detected in these fractions due to treatment of the samples with NaOH, HCl and HF. The inorganic minerals that can be identified in KB and BC are rutile, anatase and corundum. These minerals cannot be digested by HF/HCl acids. Apart from peaks associated with these minerals, a broad peak at 24.5–26° (2θ) can be found in the all spectra, representing distinct diffraction peaks of organic carbon (d_{002}) in association with the presence of condensed aromatic sheets in macromolecular matrices. It is already known that K and BC matrices have backbone structures comprising stacks of aromatic molecules and that interlayer spacing decreases as a function of condensation or maturation level of the organic matter (Yen, 1961; Qing et al., 1987).

From a closer look at Fig. 2, we find that KB contains two broad organic peaks while BC only has one peak. The low 2θ peak may correspond to diffraction of K, while the higher peak is that of BC. This assignment is consistent with the structure of K and BC. BC mainly consists of strong condensed carbon and shows a high 2θ diffraction peak.

According to $d_{002} = \lambda/2\sin\theta_{002}$, we can calculate the interlayer spacing of the aromatic structure of K and BC. Results show that BC particles in the KB and BC fractions have similar BC interlayer spacings of 0.329–0.345 nm and 0.335–0.352 nm, respectively. Interlayer spacings of K are 0.509–0.613 nm. The relatively narrow d_{002} in BC indicated that BC has more aromatic units and a more stable structure than K. In these fractions, the interlayer spacing of BC from dust in WS was 0.352 nm (d_{002}), similar to the interlayer spacing of modern BC (0.366 nm) that was isolated by Song et al. (2002), and slightly lower than the interlayer spacing of BC (0.41 nm) from vehicle exhaust (Schaefer, 2001). In conclusion, KB and BC isolated from the dust contain aromatic entities that are similar to those of graphite, but without the orderly crystal structure of graphite.

3.3. OPE

HAs, K and BC were observed under microscope with transmitted, reflected and fluorescent light modes. The resulting observations are described as follows.

3.3.1. Reflected mode

All the HA fractions from different sources had low reflectance, with colors almost the same as the background (Fig. 3A); the KB fraction contained gray “vitrinite”, yellowish “vitrinite”, semifusinite and partly bright yellow fusinite. Some of the KB fraction

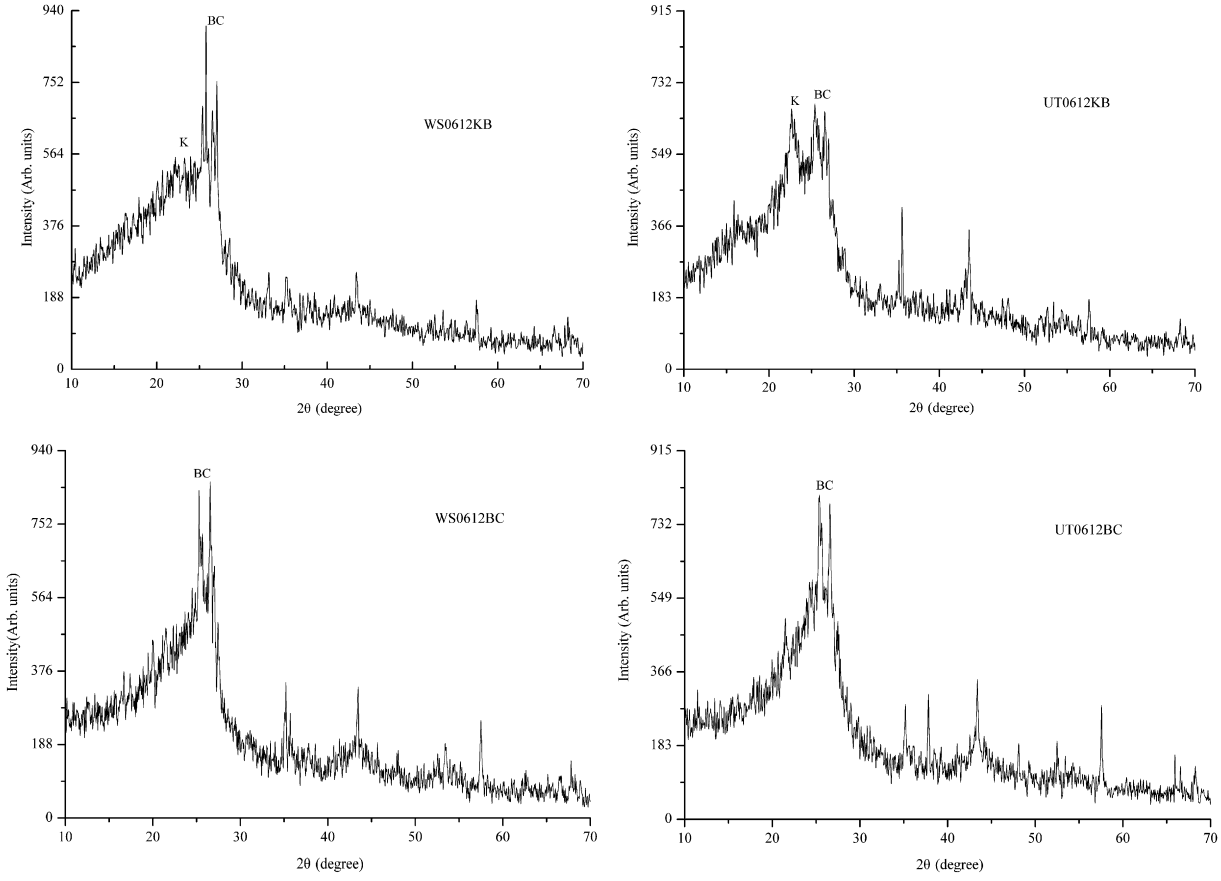

Fig. 2. XRD spectra of KBs and BCs isolated from dust in WS and UT. Note: Samples were named by site, date and fractions. For example, WS0612KB means that KB was isolated from the sample which was collected in WS in December of 2006.

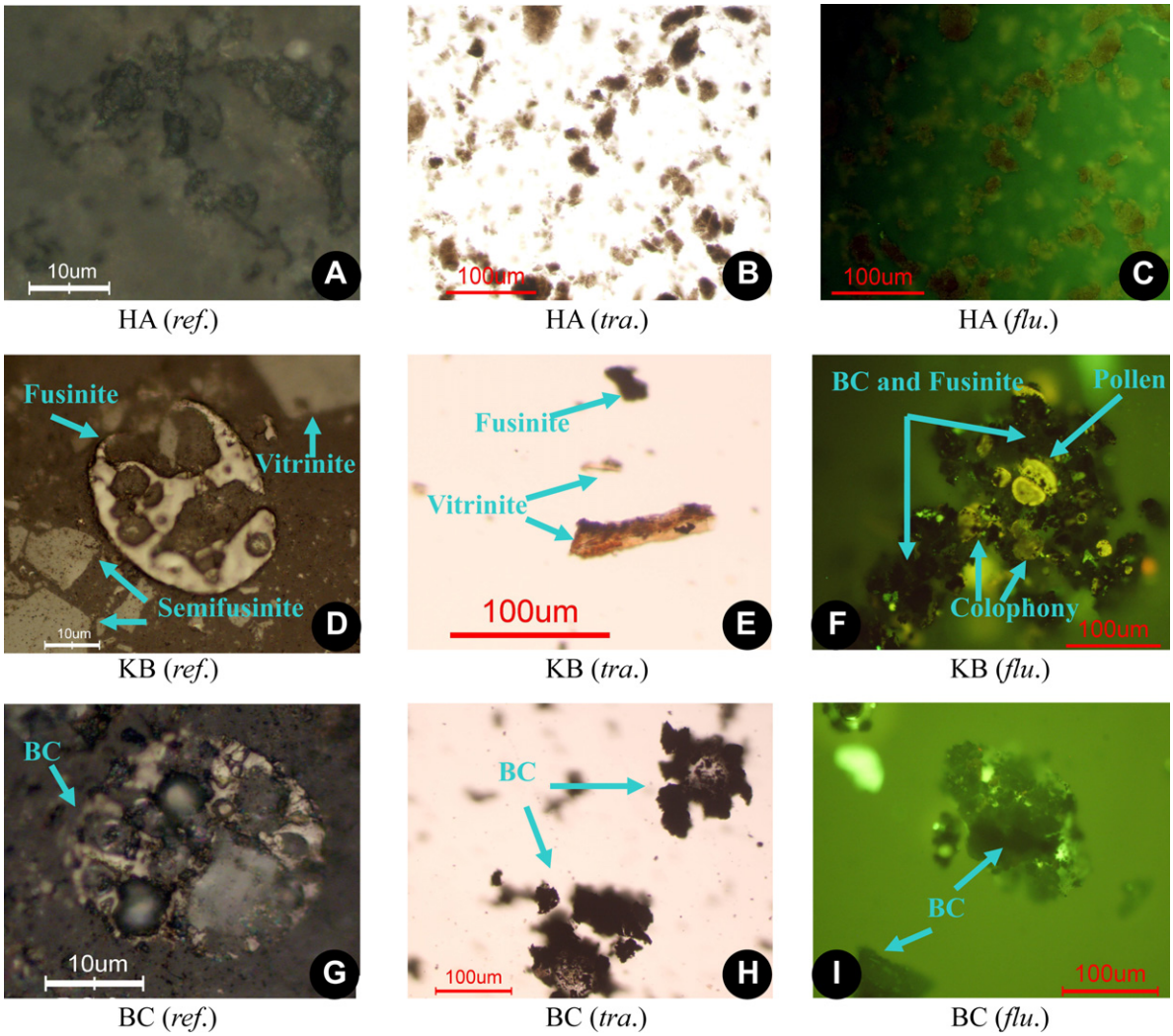

Fig. 3. Microphotographs of isolated fractions under the microscope in transmitting (*tra.*), reflecting (*ref.*) and fluorescent (*flu.*) modes. (A) Low reflectivity of HA under reflecting microscope; (B) Transparent, translucent and brown humus and amorphism organic matter under transimitting microscope; (C) No fluorescence of HA under fluorescent microscope; (D) Fusinite (BC) with high reflectance, semifusinite with median reflectance and "vitrinite" with low reflectance in KB fraction; (E) Translucent and brown "vitrinite" and opaque fusinite; (F) Bright-yellow pollen, brown-yellow colophony and opaque fusinite; (G) Fusinite with macroporous structure and "vitrinite" with low reflectance; (H) Amophism and bulbiform BC; (I) Opaque fusinite with scattered fluorescence. (For interpretation of the references to color in this figure legend, the reader is referred to the web version of this article.)

retained the clear organizational structure of plant cells (Fig. 3D). Compared with KB, components of BC were relatively simple and mainly contained bright yellow, irregular and rounded fusinite and light yellow semifusinite (Fig. 3G). Some of the BC fraction also retained the organizational structure of the plant cells (Fig. 3D and G), and was generally recognized as charcoal.

3.3.2. Transmitted mode

In this mode, the HA fraction appeared as transparent, translucent, brown-yellow and brown (Fig. 3B). The KB fraction was composed of opaque fusinite and semifusinite, dark-brown "vitrinite" and a little translucent material similar to the HAs (Fig. 3E). Meanwhile, the BC fraction mainly consisted of opaque particles, but a small quantity of brown particles were mixed in with some samples (Fig. 3H) and were identified as fusinite and semifusinite macerals.

3.3.3. Fluorescent mode

Some macerals (such as spores, epidermis) can fluoresce under excitation by blue and ultraviolet light (Karapanagioti et al., 2000). Therefore, the color and intensity of the fluorescence of excited organic matter may help identify the types of macerals. The HA fractions were colorless in this mode. The KB fraction contained more fluorescent components; these were bright-yellow pollen and brown-yellow spores (Fig. 3F). The BC fractions were generally colorless, consistent with the compositions of fusinite and semifusinite.

In terms of the chemical structures of coal macerals which have been well studied (Vandenbroucke and Largeau, 2007), we can ascribe "vitrinite" to K, and semifusinite and fusinite to BC. In the coal sample, "vitrinite" is formed by the gelation of lignins. In our case, "vitrinite" is also possibly formed by the photochemical reaction of VOCs. For the semifusinite and fusinite macerals, the geologist and environmental scientist will share the same recognition that they are derived from combustion.

3.4. SEM analysis

We only analyzed the KB and BC fractions using the SEM, because HAs contain high concentrations of free radicals and were therefore unsuitable for SEM observation.

BC particles (Fig. 4A and B) present in the samples had a unique pore structure, indicating that they were generated from organisms or from the incomplete combustion of fossil fuels (e.g., coal or oil). A closer examination shows that two types of BC particles can be distinguished. One has elongated/layered structures (Fig. 4B and E), suggesting its possible derivation from incomplete burning of plant or coal materials. The other has irregular or spheroidal features with smooth and homogeneous surfaces (Fig. 4A and C), indicating its source in oil or coal burning processes (Griffin and Goldberg, 1981).

The organic matter in the KB fraction (Fig. 4C) showed a distinct shape and clear surface features. Although HAs had been removed, they seemed to be present on the surface of KB as a coating material (Fig. 4B). In this fraction, BC and fly ash structures, as mentioned above, were also present (Fig. 4A and B).

In terms of strong electron beam reflection of inorganic minerals and a distinct EDS spectrum, the insoluble inorganic minerals such as corundum can be clearly identified in the organic matter (Fig. 4F), which is consistent with the results from XRD suggesting that rutile, corundum and other minerals were detected in the organic matter. These mineral particles are resistant to treatment by HCl and HF, and were mainly seen filling holes in particles or were absorbed in the surfaces of particles.

3.5. Solid state CP/MAS ^{13}C NMR spectroscopy

The typical ^{13}C NMR spectra of the HA, KB, and BC fractions are shown in Fig. 5. For a comparative study, the resonant peaks were classified and grouped into 7 catalogues. Peaks at 0–45, 45–63, 63–93, 93–148, 148–165, 165–187, and 187–220 ppm are aliphatic, methoxyl, hydroxyl, aromatic, oxygen-substituted aromatic, carboxylic and carbonyl carbons, respectively. The areas of these peaks were integrated for calculation of relative percentage and aromaticity. The results are listed in Table 1.

Only one HA sample collected in winter from WS was analyzed by NMR. The others had insufficient sample quantities for NMR analyses. Spectra in Fig. 5 show that more than 12 peaks were identified. High carboxyl, methoxyl and aliphatic carbon contents agree well with the elemental results discussed above, i.e., the high H/C and O/C atomic ratios. Another pronounced feature of the HA

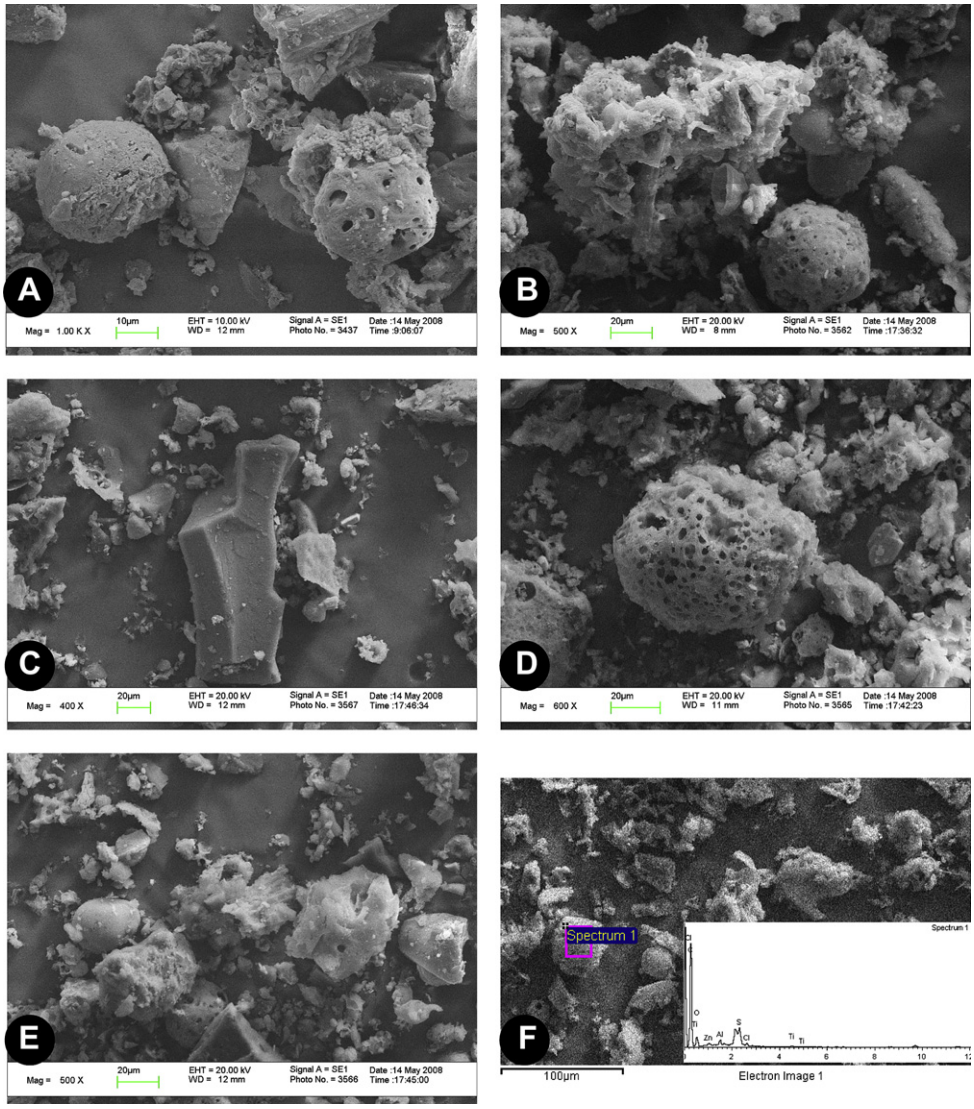

Fig. 4. Scanning electron microscopic photographs of the isolated KB and BC particles from falling dust. A, B and C: Photographs of KBs show irregular and accumulated particles (B and C), single spherical and strip-shaped BC particles (A and B), and some irregular aggregated particles that have a humus surface (B). D, E and F: Photographs of BC. They appear massive spherical, smooth surface and porous BC particles (D and E) and "vitrinite" (F). Some inorganic mineral presented in hole of BC (F), such as anatase and rutile, which were not oxidized by $H_2SO_4/K_2Cr_2O_7$.

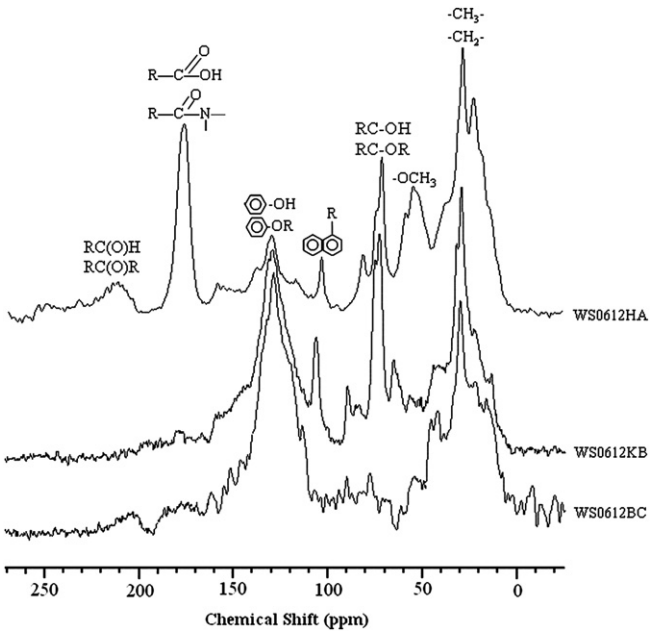

Fig. 5. CP/MAS ^{13}C NMR spectra of HA, KB and BC isolated from the dust. For the names of samples see the Fig. 2 caption.

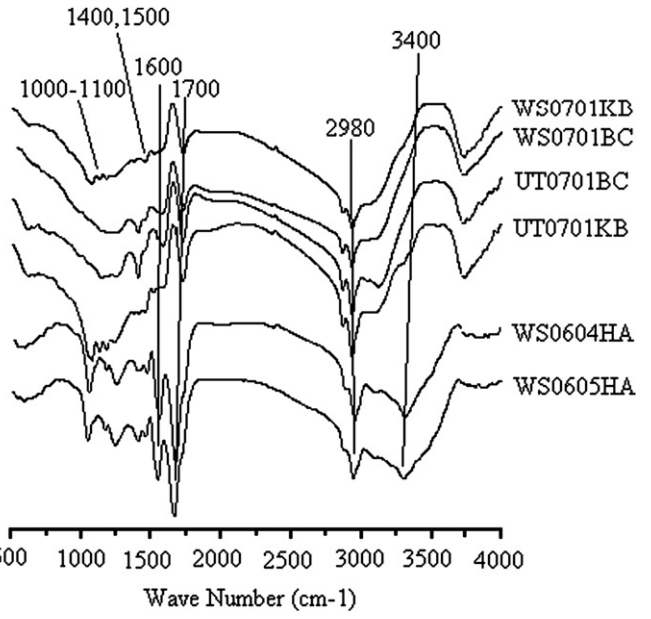

Fig. 6. FTIR spectra of the isolated fractions from the falling dust during different seasons at the WS and UT sites. Sample names follow Fig. 2.

was its low aromatic and oxygen-substituted aromatic carbon content, with an aromaticity of 23.43%. These features are similar to hulis from aerosols reported in the literature (Krivácsy et al., 2000; Sýkorová et al., 2009).

The spectra of the BC fractions are characterized by high aromatic carbon contents and substantial aliphatic and carboxyl carbon contents with aromaticity fractions of 48–60%. A little carbohydrate carbon was also present in the spectra. These characteristics are similar to results of the elemental analysis discussed above but differ slightly from modern BC derived from the combustion of fossil fuels, which completely lacks carbohydrate carbon (Petsch et al., 2001). The presence of this type of carbon in the fraction indicates that some parts of the BC are from biomass burning.

The NMR spectra of the KB fractions, shown in Fig. 5, are characterized by high aromatic, hydroxyl and aliphatic carbons with aromaticity fractions of 30–43%. If aromatic and aliphatic carbon form the basis of the BC structure, the hydroxyl carbons in KB may correspond to the structure of "vitrinite" or K. The presence of this structure is rational because "vitrinite" or K in the dust comprises oxidation products formed by inter-molecular combination process. Multi-hydroxyl and ether functional groups are characteristic of oxidation products from VOCs (Monod et al., 2005). Recently, many low molecular weight multi-hydroxyl and ether compounds were identified in total suspended particles (Ma et al., 2010; Bi et al., 2008). This structural feature further demonstrates that VOCs were not only degraded to CO_2 and H_2O but were also condensed onto solid materials such as K or "vitrinite".

If we inspect the data listed in Table S1, we can conclude: 1) aromaticity decreases in the order BC > K > HA; 2) methoxyl carbon decreases in the order HA > KB > BC; and 3) hydroxyl content is high in KB and low in HAs and BC.

3.6. FTIR spectroscopy

The FTIR analysis of HA, KB and BC may provide more information about the chemical structure which is complementary to the ^{13}C NMR results. Fig. 6 shows the FTIR spectra of selected samples, indicating that there are slight but distinct differences among the samples.

The broad band O–H peak (3600–3200 cm^{-1}) can be attributed to hydroxyl and amide stretching vibration absorption. HA samples have higher absorption peaks at 3200–3300 cm^{-1} while KB and BC have greater absorption in the 3600 cm^{-1} band. The former band

Table 1
Percentage of carbon groups in the solid ^{13}C NMR spectra.

Samples	Alkyl carbons 0–50 ppm	Methoxyl carbons 50–60 ppm	Hydroxyl carbons 60–90 ppm	Alkyl-substituted aromatic carbons 110–130 ppm	Oxygen-substituted aromatic or phenolic carbons 130–160 ppm	Carboxylic carbons 160–188 ppm	Carbonyl carbons 188–230 ppm	Aromaticity[a] (%)
UT0605KB	35.75	6.25	23.00	26.75	0.00	3.00	0.75	29.97
WS0609KB	36.12	5.07	19.40	37.31	1.19	0.59	0.00	38.74
UT0612KB	24.84	2.52	24.00	38.74	2.10	1.26	0.00	42.99
WS0612KB	34.21	0.00	18.42	39.21	0.00	1.05	0.26	41.62
UT0609BC	27.20	0.00	13.11	37.96	0.00	0.98	0.39	48.50
S0609BC	22.21	0.00	12.61	39.03	0.00	22.33	3.81	52.84
UT0612BC	33.12	3.36	2.38	55.59	2.50	3.04	0.00	59.91
WS0612BC	30.67	0.00	0.00	58.76	0.00	0.52	0.00	59.06
WS0612HA	31.80	28.45	12.92	8.94	1.12	15.90	0.87	23.43

[a] Aromaticity (%) = [aromatic C (106–150 ppm) + carboxylic C (151–170 ppm)]/[aromatic C + carboxylic C + aliphatic C (0–105 ppm)] × 100. For the names of samples see the Fig. 2 caption.

refers to OH vibration where the OH has strong inter- or intra-molecular interactions. The latter band indicates free OH vibration. Possibly, the stronger hydrogen bonds in the HA are due to carboxylic acid functional groups, which create inter-molecular linkages in HA. Meanwhile, OH in KB and BC is possibly present in the carbon structure, where inter-molecular interactions are less important than those in HA.

The absorption peaks at 2980 cm^{-1} and 2862 cm^{-1} can be classified as asymmetric and symmetric stretching vibrations of alkyl compounds. All samples contain these absorption peaks; however, HAs show relatively higher absorption at 2980 cm^{-1} and 2862 cm^{-1}. This result is consistent with the elemental and NMR analyses.

The peak at 1700 cm^{-1} is the C═O stretching vibration associated with ketones, aromatic carbon and aliphatic acids. The peak is much weaker in KB and BC than in HAs. The band at 1600 cm^{-1} is attributed to the C═C stretching vibration of aromatic rings, and is strongest in BC samples. The absorption peak at 1454 cm^{-1} is mainly due to CH_2 and CH_3 asymmetric bending vibrations. The absorption peak in BC at 1400 cm^{-1} can be attributed to C–H bending vibrations of C–$(CH_3)_2$ or C–$(CH_3)_3$ groups, indicating that there were branched-chain alkanes in the BC samples. These features are all in close agreement with the chemical structures of HA, KB and BC elucidated by NMR.

4. Conclusions

The organic macromolecules in dust can be separated into HA, KB and BC fractions by chemical manipulation. KB is the most important fraction, accounting for 64.08–95.52% of the TOC in the dust. HA is derived from photochemical reactions of VOCs and is characterized by high H/C, N/C and O/C ratios, and high carboxyl, methoxyl and aliphatic carbon in the molecular structures. K may also originate from photochemical reactions, and has a chemical composition characterized by a high hydroxyl carbon content. Visually, K appears similar to “vitrinite”. BC is formed from the combustion of biomass and fossil fuels, so that aromatic and aliphatic carbons are the most important components of its carbon skeleton. Under the microscope, BC appears as semifusinte and fusinite and has a distinct texture when observed by SEM.

Compared with the HA and K isolated from soil and sediments, HA in dust has a relatively lower aromatic ratio in its structure, and K in dust is always type III. These results agree well with the hypothesis that these materials are derived from photochemical degradation of VOCs rather than geological sources.

Acknowledgments

This work was supported by the National Natural Science Foundation of China (Nos. 40830745, 41005082 and 40975090). The authors would like to thank Miss Yu Chiling and Dr. Jia Wanglu of Guangzhou Institute of Geochemistry, CAS for their technical assistance and Dr. Shanyue Guan of Sun Yat-sen University for ^{13}C NMR measurement.

Appendix. Supplementary material

Supplementary material related to this article can be found at doi:10.1016/j.atmosenv.2011.04.039.

References

Abed, A.M., Kuisi, M.A., Khair, H.A., 2009. Characterization of the Khamaseen (spring) dust in Jordan. Atmosperic Environment 43, 2868–2876.

Bi, X.H., Simoneit, B.R.T., Sheng, G.Y., Ma, S.X., Fu, J.M., 2008. Composition and major sources of organic compounds in urban aerosols. Atmospheric Research 88, 256–265.

Dinar, E., Taraniuk, I., Graber, E.R., Katsman, S., Moise, T., Anttila, T., Mentel, T.F., Rudich, Y., 2006. Cloud condensation nuclei properties of model and atmospheric HULIS. Atmospheric Chemistry and Physics 6, 2465–2481.

Dutkiewicz, V.A., Alvi, S., Ghauri, B.M., Choudhary, M.I., Husain, L., 2009. Black carbon aerosols in urban air in South Asia. Atmosperic Environment 43, 1737–1744.

Falkovich, A.H., Schkolnik, G., Ganor, E., Rudich, Y., 2004. Adsorption of organic compounds pertinent to urban environments onto mineral dust particles. Journal of Geophysical Research 109, D02208. doi:10.1029/2003JD003919.

Garcette-Lepecq, A., Derenne, S., Largeau, C., Bouloubassi, I., Saliot, A., 2000. Origin and formation pathways of kerogen-like organic matter in recent sediments off the Danube delta (northwestern Black Sea). Organic Geochemistry 31, 1663–1683.

Goldberg, D.E., 1985. Black Carbon in the Environment: Properties and Distribution. John Wiley & Sons, New York.

Griffin, D.W., Kellogg, C.A., Garrison, V.H., Lisle, J.T., Borden, T.C., Shinn, E.A., 2003. African dust in the Caribbean atmosphere. Aerobiologia 19, 143–157.

Griffin, D.W., 2005. Clouds of desert dust and microbiology: a mechanism of global dispersion. Microbiology Today 11, 180–182.

Griffin, J.J., Goldberg, E.D., 1981. Sphericity as a characteristic of solids from fossil fuel burning in Lake Micigan sediments. Geochimica et Cosmochimica Acta 45, 763–769.

Hammes, K., Smernik, R.J., Skjemstad, J.O., Schmidt, M.W.I., 2008. Characterisation and evaluation of reference materials for black carbon analysis using elemental composition, colour, BET surface area and 13C NMR spectroscopy. Applied Geochemistry 23, 2113–2122.

Havers, N., Burba, P., Lambert, J., Klockow, D., 1998. Spectroscopic characterization of humic-like substances in airborne particulate matter. Journal of Atmospheric Chemistry 29, 45–54.

Karapanagioti, H.K., Kleineidam, S., Sabatini, D.A., 2000. Impacts of heterogeneous organic matter on phenanthrene sorption: equilibrium and kinetic studies with aquifer material. Environmental Science and Technology 34, 406–414.

Kellogg, C.A., Griffin, D.W., Garrison, V.H., Peak, K.K., Royall, N., Smith, R.R., Shinn, E.A., 2004. Characterization of aerosolized bacteria and fungi from desert dust events in Mali, West Africa. Aerobiologia 20, 99–110.

Kirchstetter, T.W., Aguiar, J., Tonse, S., Fairley, D., Nonakov, T., 2008. Black carbon concentrations and diesel vehicle emission factors derived from coefficient of haze measurements in California: 1967-2003. Atmospheric Environment 42, 480–491.

Krivácsy, Z., Kiss, G., Varga, B., Galambos, I., Sárvári, Z., Gelencsér, A., Molnára, Á., Fuzzic, S., Facchinic, M.C., Zappolid, S., Andracchiod, A., Alsberge, T., Hanssone, H.C., Perssone, L., 2000. Study of humiclike substances in fog and interstitial aerosol by size-exclusion chromatography and capillary electrophoresis. Atmospheric Environment 34, 4273–4281.

Lee, S.J., Park, H., Choi, S.D., Lee, J.M., Chang, Y.S., 2007. Assessment of variations in atmospheric PCDD/Fs by Asian dust in Southeastern Korea. Atmospheric Environment 41, 5876–5886.

Li, L., Jia, W.L., Peng, P.A., Sheng, G.Y., Fu, J.M., Huang, W.L., 2006. Compositional and source characterization of base progressively extracted humic acids using pyrolytic gas chromatography mass spectrometry. Applied Geochemistry 21, 1455–1468.

Li, L., Zhao, Z.Y., Huang, W.L., Peng, P.A., Sheng, G.Y., Fu, J.M., 2004. Characterization of humic acids fractionated by ultrafiltration. Organic Geochemistry 35, 1025–1037.

Lim, B., Cachier, H., 1996. Determination of black carbon by chemical oxidation and thermal treatment in recent marine and lake sediments and cretaceous-tertiary clays. Chemical Geology 131, 143–154.

Ma, S.X., Peng, P.A., Song, J.Z., Bi, X.H., Zhao, J.P., He, L.L., 2010. Seasonal and spatial changes of free and bound organic acids in total suspended particles in Guangzhou, China. Atmosperic Environment 44, 5460–5467.

Mafra, A.L., Senesi, N., Brunetti, G., Miklos, A.A.W., Melfi, A.J., 2007. Humic acids from hydromorphic soils of the upper Negro river basin, Amazonas: chemical and spectroscopic characterization. Geoderma 138, 170–176.

Monod, A., Poulain, L., Grubert, S., Voisin, D., Wortham, H., 2005. Kinetics of OH-initiated oxidation of oxygenated organic compounds in the aqueous phase: new rate constants, structure–activity relationships and atmospheric implications. Atmospheric Environment 39, 7667–7688.

Mukai, A., Ambe, Y., 1986. Characterization of humic acid-like brown substance in airborne particulate matter and tentative identification of its origin. Atmospheric Environment 20, 813–819.

Petsch, S.T., Smernik, R.J., Eglinton, T.I., Oades, J.M., 2001. A solid state ^{13}C-NMR study of kerogen degradation during black shale weathering. Geochimica et Cosmochimica Acta 65, 1867–1882.

Prospero, J.M., Lamb, P.J., 2003. African droughts and dust transport to the Caribbean: climate change implications. Science 302, 1024–1027.

Qing, K.Z., Zhang, X.Y., Lao, Y.X., 1987. X-ray diffraction studies of Kerogen. Acta Sedimentologica Sinica 5, 26–36.

Ran, Y., Sun, K., Yang, Y., Xing, B.S., Zeng, E., 2007. Strong sorption of phenanthrene by condensed organic matter in soils and sediments. Environmental Science and Technology 41, 3952–3958.

Salama, A., Bauera, H., Kassina, K., Ullahb, S.M., Puxbauma, H., 2003. Aerosol chemical characteristics of a mega-city in Southeast Asia (Dhaka–Bangladesh). Atmospheric Environment 37, 2517–2528.

Schaefer, A., 2001. Does supersorbent soot control PAH fate? Environmental Science and Technology 35, 10A.
Shen, Z.X., Cao, J.J., Arimoto, R., Han, Z.W., Zhang, R.J., Han, Y.M., Liu, S.X., Okuda, T., Nakao, S., Tanaka, S., 2009. Ionic composition of TSP and PM2.5 during dust storms and air pollution episodes at Xi'an, China. Atmospheric Environment 43, 2911–2918.
Simpson, M.J., Hatcher, P.G., 2004. Overestimates of black carbon in soils and sediments. Naturwissenschaften 91, 436–440.
Smith, G.W., Ives, L.D., Nagelkerken, I.A., Ritchie, K.B., 1996. Caribbean sea-fan mortalities. Nature 383, 487.
Song, J.Z., Peng, P.A., Huang, W.L., 2005. Characterization of humic acid-like material isolated from the humin fraction of a topsoil. Soil Science 170, 599–611.
Song, J.Z., Peng, P.A., Huang, W.L., 2002. Black carbon and kerogen in soils and sediments. 1. Quantification and characterization. Environmental Science and Technology 36, 3960–3967.
Sullivan, R.C., Guazzotti, S.A., Sodeman, D.A., Tang, Y., Carmichael, G.R., Prather, K.A., 2007. Mineral dust is a sink for chlorine in the marine boundary layer. Atmospheric Environment 41, 7166–7179.
Sýkorová, I., Havelcová, M., Trejtnarová, H., Matysová, P., Vašíček, M., Kříbek, B., Suchý, V., Kotlík, B., 2009. Characterization of organic matter in dusts and fluvial sediments from exposed areas of downtown Prague, Czech Republic. International Journal of Coal Geology 80, 69–86.
Taraniuk, I., Graber, E.R., Kostinski, A., Rudich, Y., 2007. Surfactant properties of atmospheric and model humic-like substances (HULIS). Geophysical Research Letters 34, L16807. doi:10.1029/2007GL029576.
Vandenbroucke, M., Largeau, C., 2007. Kerogen origin, evolution and structure. Organic Geochemistry 38, 719–833.
Weir-Brush, J.R., Garrison, V.H., Smith, G.W., Shinn, E.A., 2004. The relationship between gorgonian coral (Cnidaria: Gorgonacea) diseases and African dust storms. Aerobiologia 20, 119–126.
Yen, T.F., 1961. Structural investigation in Green River oil shale kerogen. In: Science and Technology of Oil Shale, pp. 193–205. Ann Arbor, New York.
Zappoli, S., Andracchio, A., Fuzzi, S., Facchini, M.C., Gelencser, A., Kiss, G., Krivácsy, Z., Molnár, Á, Mészáros, E., Hansson, H.C., Rosman, K., Zebühr, Y., 1999. Inorganic, organic and macromolecular components of fine aerosol in different areas of Europe in relation to their water solubility. Atmospheric Environment 33, 2733–2743.
Zhao, J.P., Peng, P.A., Song, J.Z., Ma, S.X., Sheng, G.Y., Fu, J.M., 2010. Research on flux of dry atmospheric falling dust and its characterization in a subtropical city, Guangzhou, South China. Air Quality, Atmosphere and Health 3, 139–147.